J Mater Sci: Mater Electron (2013) 24:2339–2345
DOI 10.1007/s10854-013-1098-1

Comparative study on mechanical properties of undoped and Ce-doped Bi-2212 superconductors

Y. Zalaoglu · E. Bekiroglu · M. Dogruer · G. Yildirim · O. Ozturk · C. Terzioglu

Received: 6 December 2012 / Accepted: 19 January 2013 / Published online: 29 January 2013

Abstract This study discusses the mechanical performances of $Bi_{1.8}Sr_{2.0}Ce_xCa_{1.1}Cu_{2.1}O_y$ ceramics with x = 0, 0.001, 0.003, 0.005, 0.01, 0.03, 0.05 and 0.1 by way of Vickers microhardness (H_v) measurements performed at different applied loads in the range of 0.245–2.940 N. For the potential industrial applications, the important mechanical characteristics such as Vickers microhardness, elastic modulus, yield strength, fracture toughness and brittleness index values of the samples studied are extracted from the microhardness measurements. All the results obtained indicate that the Vickers hardness, Young's (elastic) modulus, yield strength, fracture toughness and brittleness index values suppress with the increment of the Ce concentration in the system as a consequence of the degradation in the connectivity between superconducting grains. The decrement in the H_v values with the applied load is attributed Indentation Size Effect behaviour of the samples studied. Moreover, the experimental results of Vickers microhardness measurements are estimated using the 5 different models such as Kick's law, proportional sample resistance model, modified proportional sample resistance model, elastic/plastic deformation model and Hays–Kendall approach. According to the results obtained from the simulations, Kick's law is not useful model to obtain information about the origin of the indentation size effect feature of the Ce-doped bulk Bi-2212 superconductors. On the other hand, the Hays–Kendall approach is determined as the most suitable model for the description of the mechanical properties of the superconducting samples. In addition, the bulk porosity analysis for the samples reveals that the porosity increases monotonously with the Ce inclusion in the Bi-2212, leading to the degradation of the grain connectivity.

Y. Zalaoglu · E. Bekiroglu · M. Dogruer · G. Yildirim · C. Terzioglu (✉)
Department of Physics, Abant Izzet Baysal University, 14280 Bolu, Turkey
e-mail: terzioglu_c@ibu.edu.tr

Y. Zalaoglu
Department of Physics, Osmaniye Korkut Ata University, 80000 Osmaniye, Turkey

E. Bekiroglu
Department of Electrical and Electronic Engineering, Abant Izzet Baysal University, 14280 Bolu, Turkey

G. Yildirim
Department of Mechanical Engineering, Abant Izzet Baysal University, 14280 Bolu, Turkey

O. Ozturk
Department of Physics, Kastamonu University, 37100 Kastamonu, Turkey

1 Introduction

For the bulk superconductor materials, the mechanical characteristics being closely related with their other physical, electrical, microstructural and superconducting properties are useful to determine the performance of devices prepared from the solids. Microhardness testing is commonly used to evaluate the mechanical properties and strongly related to the composition and structure of the samples studied. Thus, it is not wrong to say that the hardness tests are popular to characterize the materials for the industrial applications [1–4]. The conventional method of microhardness measurement contains two parts: (I) application of a fixed load on a diamond indenter and (II) determination of the dimension of the resultant indentation on the specimen surface. Several studies performed show that the Vickers hardness of a sample is related to a function of the applied load [5, 6].

The Vickers hardness values of different applied loads are calculated by means of the equation given below:

$$H_V = 1854.4\left(\frac{F}{d^2}\right) \quad (1)$$

where H_v (GPa) represents the Vickers hardness, d (μm) denotes diagonal length of indentation and F(N) is the applied load. A sample exhibits either an indentation size effect (ISE) or reverse indentation size effect (RISE) behavior with regard to the microstructural properties. For the former one, the hardness values reduce with the increase in the applied load due to the weak grain boundaries, impurity phases and irregular grain orientation distribution [7, 8]. Hence, both elastic and plastic deformation are observed in the material. On the other hand, the important characteristic for the latter feature is attributed to the fact that the microhardness values ascend with the increase of the applied load [9] owing to the presence of the specimen cracking. Unlike the ISE behavior, the plastic deformation becomes more and more dominant compared to the elastic deformation. In the current work, all the samples prepared exhibit the ISE behaviour.

The elastic (Young's) modulus (E), yield strength (Y), fracture toughness (K_{IC}) and brittleness index (B) properties obtained from the Vickers microhardness measurement results of the studied sample are computed by means of Eqs. [10–12]:

$$E = 81.9635H_V \quad (2)$$

$$Y \approx \frac{H_V}{3} \quad (3)$$

$$K_{IC} = \sqrt{2E\gamma} \quad (4)$$

$$B = \frac{H_v}{K_{IC}} \quad (5)$$

In order to examine ISE nature of the samples, Meyer's law can be defined by following Eqs. [13, 14]

$$F = A_1 d^n \quad (6)$$

where the power n presents the Meyer number obtained from the fitted curves of the experimental data, and A_1 denotes the standard hardness constant. When the value of $n < 2$, the microhardness values decrease with the increase of the applied load (the basic characteristic of ISE behaviour). In the case of $n > 2$, the microhardness enhances with increasing the applied load (the basic characteristic of *RISE* behaviour). However, the hardness is independent of applied load when $n = 2$ and in this case the relation between applied load and diagonal indentation is given by $F = A_1 d^2$ (Kick's law). In most cases, Kick's law is hardly met because the exponent n is generally less or larger than 2.

The proportional specimen resistance (PSR) model is conducted on several materials to calculate the ISE behaviour [15]. According to the literature, the PSR can be described by the following equation

$$\frac{F}{d} = \alpha + \beta d \quad (7)$$

The coefficients of α (displaying the surface energy) and β (a parameter used to compute the load independent microhardness value) are related to the calculation of the load independent microhardness values. The hardness value is governed by

$$H_{PSR} = 1854.4\beta \quad (8)$$

Modified proportional specimen resistance model has recently been proposed to examine the ISE behavior. According to the model, this behaviour can be defined by the Eq. [16]:

$$F = W_1 + A_2 d + A_3 d^2 \quad (9)$$

where W_1 corresponds to minimum applied load to generate an indentation when A_2 and A_3 are associated with the dissipation energies to create a new surface of a unit area and produce the permanent deformation of a unit volume. Based on the MPSR model, for the micro-indentation test with a Vickers indenter, true hardness, H_{MPSR}, can be determined directly by the equation

$$H_{MPSR} = 1854.4A_3 \quad (10)$$

Bull et al. [17] proposed that the dependence of indentation size on the applied load can be obtained by way of equation:

$$F = A_4(d_e + d_p)^2 \quad (11)$$

Here A_4 denotes constant, and d_e is related on the d_p. Then, the load independent microhardness (H_{EPD}) values are expressed by means of the following equation:

$$H_{EPD} = 1854.4A_4 \quad (12)$$

Hays–Kendall (HK) approach displays that there exists a minimum specimen resistance to initiate plastic deformation and below which only elastic deformation is occurred in the studied samples for applied load [18]. HK found that indentation size is proportional to an effective load $F_{eff} = F - W_2$ rather than the applied load

$$F - W_2 = A_5 d^2 \quad (13)$$

where A_5 is the hardness constant and W_2 denotes sample resistance pressure. Thus, H_{HK} can be computed by use of the following equation:

$$H_{HK} = 1854.4A_5 \quad (14)$$

The values of W_2 and A_5 can be calculated plotting the applied load (F) as against indentation size (d^2) graphs.

The Indentation-Induced cracking (IIC) model is another approach used recently to investigate the RISE

behavior of various materials [19, 20]. In this model, the applied load is balanced by the total specimen resistance at the maximum depth composed of four components due to the friction at the indenter or specimen facet interface (frictional component), elastic deformation, plastic deformation and specimen cracking. According to IIC model, indentation cracking contributes to the RISE feature whereas frictional and elastic effects lead to the ISE behaviour of a sample studied. The load independent microhardness value (H_{IIC}) can be computed by using the following equation:

$$H_v = \lambda_1 K_1 \left(\frac{F}{d^2}\right) + K_2 \left(\frac{F^{5/3}}{d^3}\right) \quad (15)$$

where λ_1, K_1 and K_2 are constants.

In this study, we report the influence of the mechanical properties of Ce addition in the Bi-2212 ceramics by means of Vickers microhardness (H_v) measurements. The results of the microhardness measurements are examined by different available models such as Meyer's law, PSR, MPSR, EPD and HK model. The HK approach is found to be the best model defining the microhardness of the Ce-doped Bi-2212. Additionally, we calculate porosity values from the density results to discuss the relationship between the mechanical properties and grain connectivity between superconducting grains.

2 Experimental details

In previous work [21], we investigated the function of Cerium (Ce) inclusions on electrical, structural, physical and superconducting properties of the Bi-2212 superconductors by the way of electrical resistance (R–T), X-ray analysis (XRD), scanning electron microscopy (SEM), transport critical current density (J_c) and electron dispersive X-Ray (EDX) measurements in detail. Moreover, the examination of the flux pinning mechanism properties in the applied magnetic fields range of 0–7 T was the continuation of the systematic study on the characterization of the samples [22]. In this work, using the same samples, the role of Ce doped in Bi-2212 system on mechanical properties is examined by way of Vickers microhardness (H_v) measurements. Shimadzu HVM-2 model digital microhardness tester is used for the microhardness measurements of the samples studied. The applied load is varied from 0.245 to 2.940 N for a loading time of 10 s and accuracy in the determination of indentation diagonals is measured to be ±0.1 μm. The indenter is pressed on the different locations on the specimen surface to avoid surface effects and work hardening. An average of five readings at different locations of the specimen surfaces is taken to obtain reasonable mean values for each load. Some important mechanical properties (Vickers microhardness, elastic modulus, yield strength, fracture toughness and brittleness index) for the industrial applications of the superconductor materials are deduced from the Vickers microhardness measurement results. Here, the undoped sample is visualized as Ce0 while the superconductor samples produced with different Ce concentration such as 0.001, 0.003, 0.005, 0.01, 0.03, 0.05 and 0.1 will be herein after denoted as Ce0, Ce1, Ce3, Ce4, Ce5, Ce6 and Cu7, respectively. At the same time, the porosity for all the samples is determined from the density results obtained from [21] and the strength of connection between superconducting grains is discussed in detail.

3 Result and discussion

3.1 Microhardness and modeling

The indentation diagonal lengths as a function of the test load are measured to examine the evaluation of the mechanical properties of the Ce-doped Bi-2212 superconducting materials (Fig. 1). The measured indentation lengths and load dependent microhardness (H_v) values computed using Eq. (1) for different applied loads (0.245 N ≤ F ≤ 2.940 N) are tabulated in Table 1. As can be easily seen from the table, the hardness values for all the samples depend sensitively on ISE and applied loads. The microhardness values of Ce0, Ce1, Ce2, Ce3, Ce4, Ce5, Ce6, Ce7 samples at the constant load of 2.94 N are obtained to be about 0.667, 0.533, 0.453, 0.395, 0.326, 0.253, 0.199 and 0.159 GPa, respectively. Based on these results, the H_v values are found to reduce with the increase of the applied load and Ce addition in Bi-2212 system. It is

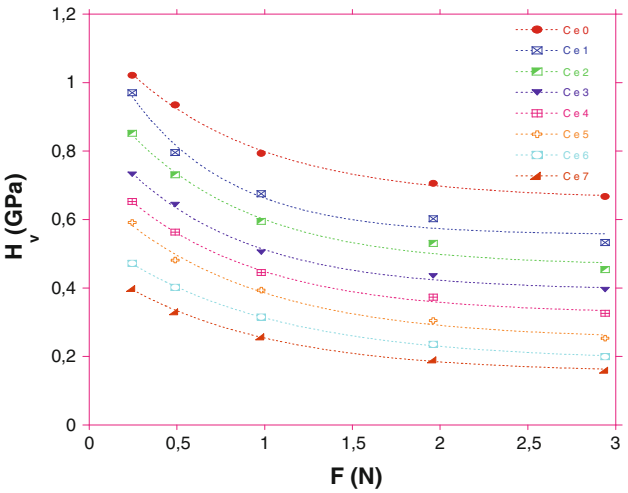

Fig. 1 Variation of load dependent microhardness H_v with applied load F for all samples

Table 1 The calculated load dependent H_v, E, Y, K_{IC} and B for the samples produced

Samples	F(N)	H_v (GPa)	E (GPa)	Y (GPa)	K_{IC} (Pa/m$^{1/2}$)	B (μm$^{1/2}$)
Ce0	21.09	1.021	83.684	0.340	1.001	1.010
	31.18	0.934	76.553	0.311	0.957	0.966
	47.85	0.793	64.997	0.264	0.882	0.890
	71.76	0.705	57.784	0.235	0.832	0.839
	90.38	0.667	54.669	0.222	0.809	0.816
Ce1	21.64	0.970	79.504	0.323	1.042	0.984
	33.79	0.795	65.160	0.265	0.944	0.891
	51.88	0.675	55.325	0.225	0.870	0.821
	77.67	0.602	49.342	0.200	0.821	0.775
	101.12	0.533	43.686	0.177	0.773	0.730
Ce2	23.09	0.852	69.832	0.284	0.987	0.923
	35.27	0.730	59.833	0.243	0.913	0.854
	55.27	0.594	48.686	0.198	0.824	0.770
	82.78	0.530	43.440	0.176	0.778	0.728
	109.62	0.453	37.129	0.151	0.719	0.673
Ce3	24.91	0.732	59.997	0.244	0.881	0.855
	37.56	0.644	52.784	0.214	0.826	0.802
	60.02	0.504	41.309	0.168	0.731	0.709
	91.38	0.435	35.654	0.145	0.679	0.659
	117.43	0.395	32.375	0.131	0.647	0.628
Ce4	26.38	0.652	53.440	0.217	0.843	0.807
	40.17	0.563	46.145	0.187	0.783	0.750
	63.90	0.445	36.473	0.148	0.696	0.667
	98.69	0.373	30.572	0.124	0.637	0.610
	129.30	0.326	26.720	0.108	0.596	0.570
Ce5	27.71	0.591	48.440	0.197	0.832	0.768
	43.44	0.481	39.424	0.160	0.750	0.693
	67.94	0.393	32.211	0.131	0.678	0.626
	109.18	0.304	24.916	0.101	0.596	0.551
	146.58	0.253	20.736	0.084	0.544	0.502
Ce6	31.01	0.472	38.686	0.157	0.716	0.687
	47.56	0.401	32.867	0.133	0.660	0.633
	75.95	0.315	25.818	0.105	0.585	0.561
	124.23	0.235	19.261	0.078	0.505	0.484
	165.24	0.199	16.310	0.066	0.465	0.446
Ce7	33.76	0.398	32.621	0.132	0.636	0.630
	52.43	0.330	27.047	0.110	0.580	0.574
	84.06	0.257	21.064	0.085	0.511	0.506
	138.23	0.190	15.573	0.063	0.440	0.435
	184.73	0.159	13.032	0.053	0.402	0.398

another interesting result from Fig. 1 that the rapid change in the H_v values is found with enhancing applied load from 0.245 to 2.000 N and after this point, it tends to reach plateau (saturation) region. The reason for this behavior is due to the contribution of weak grain boundaries, impurity phases and irregular grain orientation distribution [23]. This non-linear behavior is known as the ISE [24].

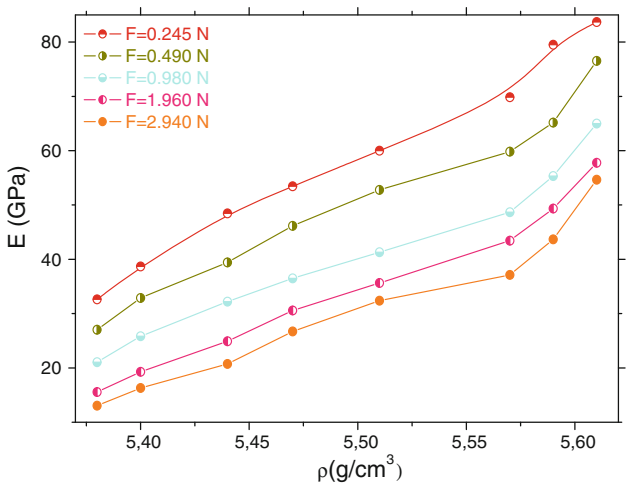

Fig. 2 Variation of E with ρ at different applied loads for all the samples

The values of load dependent E, Y, K_{IC} and B are calculated for each load by using Eqs. (2)–(5) and the results obtained are displayed in Table 1. It is apparent from the table, the load dependent E, Y, K_{IC} and B values decrease with ascending the applied loads and Ce addition owing to the crack initiation of microhardness. As well known, the change (increment/decrement) in E, Y and K_{IC} values corresponds to the average surface energy of the samples. Additionally, variation of the E values as a function of the bulk density (Fig. 2) is another interesting clue to discuss the connectivity between superconducting grains in the Ce-doped Bi-2212 materials. One can see from the figure that although the greatest E values belong to the pure (Ce0) sample at each applied load, the values tend to reduce with the decrement of the bulk densities which may be attributed to a significant decrement in the grain size, have been supported by the SEM and XRD investigations elsewhere [21]. Furthermore, several relationships between the applied load and the indentation diagonal length to explain the ISE behavior of the samples studied are discussed in the following models.

3.1.1 *Meyer's law*

The variation of applied load *lnF* with respect to the diagonal *lnd* for all the superconducting samples is reported in Fig. 3. The slope of the graph is proportional to n when A_1 can be obtained from the vertical intercept of the curve. From lnF versus lnd curves, spontaneous Meyer number (n) and standard hardness constant (A_1) values are determined for the samples and gathered in Table 2. It is visible from the table that the n values of the samples gradually decrease from 1.69 to 1.45 with the increment of

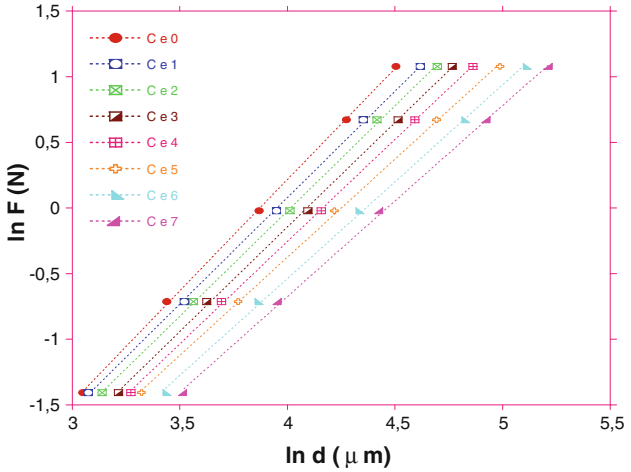

Fig. 3 Variation of applied load *lnF* with diagonal *lnd* for the samples

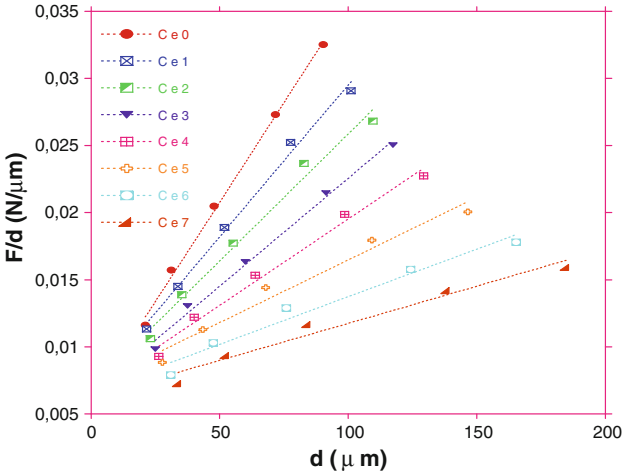

Fig. 4 Plots of F/d versus d for the samples studied

the Ce addition in the Bi-2212 system. The Ce0 sample has the maximum n value whereas the smallest value is observed for the Ce7 sample.

3.1.2 Proportional specimen resistance (PSR) model

Figure 4 demonstrates F/d versus d graph for the all the samples produced. The value of surface energy (α) and β parameter (being used to compute the load independent microhardness value) can be obtained for the different Ce content. While the β values are found to decrease systematically with the applied loads and concentration level, the change of the α values is obtained randomly for the samples produced (Table 2).

3.1.3 Modified PSR (MPSR) model

Comparisons made between applied loads and indentation diagonal lengths with regard to Ce contents in the Bi-2212 system are visualized in Fig. 5. The calculated values of W_1, A_2 and A_3 are listed in Table 2. As can be seen from the table, the A_3 values are obtained to decrease with the increase of both the applied load and Ce inclusions inserted in Bi-2212 system.

3.1.4 Elastic/plastic deformation (EPD) model

Figure 6 depicts applied load dependence of the indentation diagonal length ($F^{1/2}$ vs. d plots). Analyses of the data are presented in Table 2. It is visible from the table that the value of de is found to be positive for all the Ce-doped Bi-2212 materials, ($0 \leq x \leq 0.1$), meaning that the elastic deformation is observed along with the plastic deformation. This phenomenon results from the ISE behavior of the samples. Besides, the values of A_4 are noted to reduce with ascending the level of Ce addition (Table 2).

3.1.5 Hays–Kendall approach

The change of the applied load with the square of the indentation diagonal lengths is illustrated in Fig. 7.

Table 2 The calculated parameters according to different models for Bi-2212

Samples	Meyer's law		PSR model		MPSR model			EPD model		HK model	
	$A_1 \times 10^{-3}$ (N/μm^2)	n	$\alpha \times 10^{-3}$ (N/μm)	$\beta \times 10^{-4}$ (N/μm^2)	W_1 (N)	$A_2 \times 10^{-3}$ N/μm)	$A_3 \times 10^{-4}$ (N/μm^2)	d_e (μm)	$A_4 \times 10^{-3}$ (N/μm^2)	W_2 (N)	$A_5 \times 10^{-4}$ (N/μm^2)
Ce0	1.401	1.69	5.993	2.962	0.055	8.833	2.687	0.143	17.468	0.144	3.459
Ce1	2.151	1.62	6.841	2.265	0.132	12.918	1.741	0.177	15.423	0.187	2.761
Ce2	1.606	1.60	6.979	1.889	0.182	14.833	1.260	0.193	14.148	0.211	2.344
Ce3	1.483	1.59	6.475	1.609	0.077	9.678	1.167	0.194	13.084	0.219	2.028
Ce4	1.511	1.55	6.650	1.288	0.139	11.936	0.923	0.214	11.794	0.226	1.668
Ce5	1.730	1.49	7.148	0.932	0.200	14.126	0.501	0.252	10.222	0.276	1.285
Ce6	1.589	1.47	6.642	0.708	0.169	11.989	0.413	0.262	8.979	0.282	1.006
Ce7	1.502	1.45	6.219	0.552	0.167	10.998	0.315	0.271	7.990	0.291	0.803

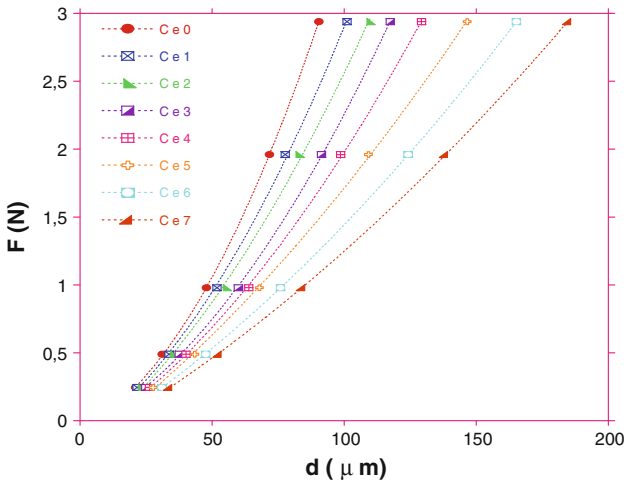

Fig. 5 Variation of applied load with the indentation diagonal length for the samples

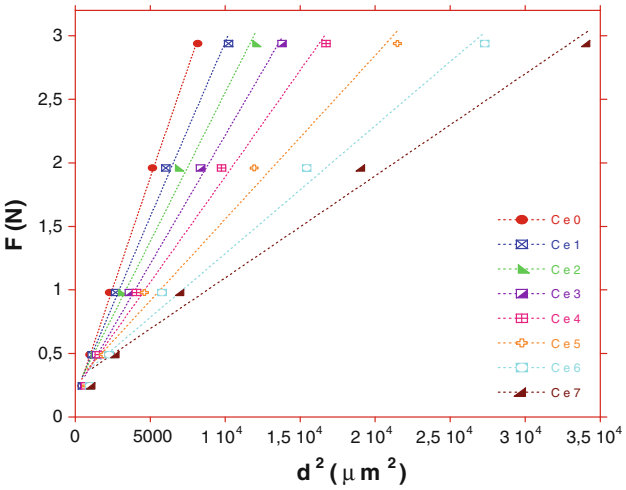

Fig. 7 Applied load versus the square of the impression length for the samples prepared

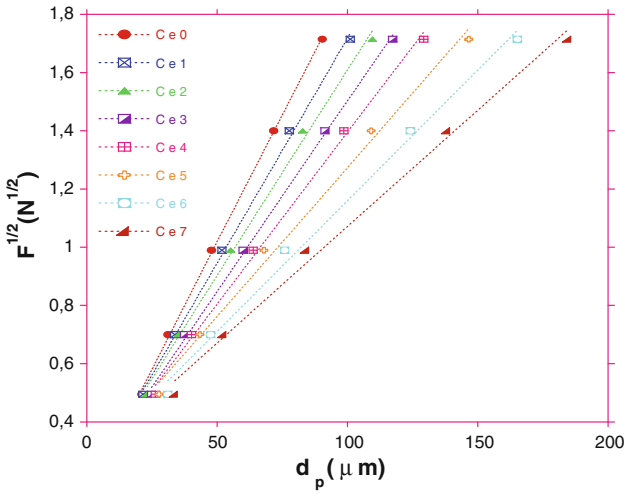

Fig. 6 Plots of square root of applied loads versus diagonal length for the samples

When the resistance pressures (W_2) are obtained to enhance with increasing applied load and Ce content, the load independent hardness constant (A_5) values are found to reduce with the increase of applied load (Table 2). Moreover, it is clear from the table that the maximum A_5 is found to be about 3.459×10^{-4} (N/μm^2) for the Ce0 sample whereas the minimum value of 0.803×10^{-4} (N/μm^2) is observed for the Ce7 sample.

The results obtained from microhardness analyses are reported in Table 3. It is visible from the table that the Kick's law is not valid for the present samples since Meyer number (*n*) is obtained to be less than 2 for all the samples studied, presenting that the behavior of the materials undergoes ISE. Further, the calculated H_V values are far from the H_{PSR}, H_{EPD} and H_{MPSR} values, confirming that the PSR, EPD and MPSR models are not adequate for the determination of the real microhardness values of the samples prepared. In addition, the best model depicting the Vickers microhardness of $Bi_{1.8}Sr_{2.0}Ce_xCa_{1.1}Cu_{2.1}O_y$ samples is found to be the Hays–Kendall approach.

3.2 The porosity analyses

With the aid of the density results obtained from [21], the porosity values described as the degree of granularity are computed by the two methods [16, 25] to discuss the strength of connection between superconducting grains. The porosity value of Ce0, Ce1, Ce2, Ce3, Ce4, Ce5, Ce6,

Table 3 The results of calculated values of H_V, H_{PSR}, H_{MPSR}, H_{EPD}, and H_{HK} model

Samples	H_{MPRS} (GPa)	H_{PSR} (GPa)	H_{EPD} (GPa)	H_{HK} (GPa)	H_V (GPa)
Ce0	0.498	0.549	0.565	0.641	0.667–0.705
Ce1	0.322	0.420	0.441	0.512	0.533–0.602
Ce2	0.233	0.350	0.371	0.434	0.453–0.530
Ce3	0.216	0.298	0.317	0.376	0.395–0.435
Ce4	0.171	0.238	0.257	0.309	0.326–0.373
Ce5	0.092	0.172	0.193	0.238	0.253–0.304
Ce6	0.076	0.131	0.149	0.186	0.199–0.235
Ce7	0.058	0.102	0.118	0.148	0.159–0.190

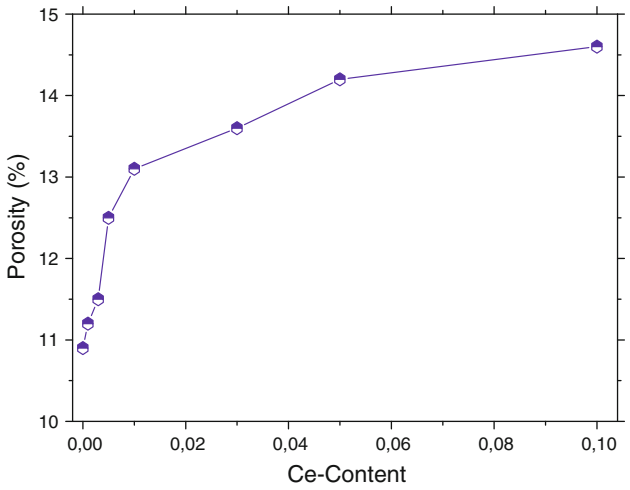

Fig. 8 Variation of porosity with Ce-content for Bi-2212 system

Ce7 samples is obtained to be about 10.9, 11.2, 11.5, 12.5, 13.1, 13.6, 14.2 and 14.6, respectively. As presented in Fig. 8, the porosity values increase with the enhancement of the Ce content in the system and in fact the Ce7 sample has the largest pores along with the weakest connection between the superconducting grains, showing that why the mechanical properties of the samples studied restrain with the content.

4 Conclusion

In this study, the role of Ce content on the mechanical properties of $Bi_{1.8}Sr_{2.0}Ce_xCa_{1.1}Cu_{2.1}O_y$ superconductors prepared by the conventional solid-state reaction with $x = 0$, 0.001, 0.003, 0.005, 0.01, 0.03, 0.05 and 0.1 is analyzed via Vickers microhardness, H_v, measurements. The Vickers hardness, Young's modulus, yield strength, fracture toughness and brittleness index values are deduced from the H_v measurements. Moreover, the Vickers microhardness results allow us to derive the mechanical properties of the superconducting samples using the Meyer's law, proportional sample resistance (PSR), modified PRS (MPSR), Elastic–Plastic deformation model (EPD) and Hays–Kendall (HK) approach. Based on the simulations, all the models expect for the Hays–Kendall approach fail to describe the ISE behavior of the Ce-doped Bi-2212 system. In other words, the dependence of Vickers microhardness for the samples on the applied load is best fitted with the HK approach. The porosity values determined from the bulk density values are also examined for the grain connectivity in the materials. The relationship between the mechanical properties and grain connectivity shows that the decrease in the mechanical properties with the enhancement of the Ce individuals in the system stems from the degradation in the connectivity between superconducting grains.

References

1. Y. Yoshino, A. Iwabuchi, R. Onodera, A. Chiba, K. Katagiri, T. Shimizu, Cryogenics **41**, 505 (2001)
2. E. Asikuzun, O. Ozturk, H.A. Cetinkara, G. Yildirim, A. Varilci, M. Yılmazlar, C. Terzioglu, J. Mater. Sci.: Mater. Electron. (2011). doi:10.1007/s10854-011-0537-0
3. O. Uzun, T. Karaaslan, M. Keskin, J. Alloy. Compd. **358**, 104 (2003)
4. O. Uzun, U. Kolemen, S. Çelebi, N. Güçlü, J. Eur. Ceram. Soc. **25**(6), 969 (2005)
5. C. Terzioglu, J. Alloy. Compd. **509**, 87 (2011)
6. J. Gong, J. Wu, Z. Guan, Mater. Lett. **38**, 197 (1999)
7. M. Dogruer, O. Gorur, Y. Zalaoglu, O. Ozturk, G. Yildirim, A. Varilci, C. Terzioglu, J. Mater. Sci.: Mater. Electron. (2012). doi:10.1007/s10854-012-0755-0
8. A.A. Elmustafa, D.S. Stone, J. Mech. Phys. Solid **51**, 357 (2003)
9. R. Awad, A.I. Abou Aly, M. Kamal, M. Anas, J. Supercond. Nov. Magn. **24**, 1947 (2011)
10. C. Veerender, V.R. Dumke, M. Nagabhooshanam, Phys. Status Solidi (a) **144**, 299 (1994)
11. M. Dogruer, G. Yildirim, O. Ozturk, A. Varilci, N. Soylu, O. Gorur, C. Terzioglu, J. Mater. Sci.: Mater. Electron. (2012). doi:10.1007/s10854-012-0917-0
12. R.W. Davidge, *Mechanical Behavior of Ceramics* (Cambridge University Press, Cambridge, 1979), pp. 31–50
13. M. Dogruer, G. Yildirim, O. Ozturk, C. Terzioglu, J. Supercond. Nov. Magn. (2012). doi:10.1007/s10948-012-1719-6
14. H. Wang, A. Serquis, B. Maiorov, L. Civale, Q.X. Jia, P.N. Arendt, S.R. Foltyn, J.L. Macmanus-Driscoll, X. Zhang, J. Appl. Phys. **100**, 053904 (2006)
15. M. Nursoy, M. Yilmazlar, C. Terzioglu, I. Belenli, J. Alloys Compd. **459**, 399 (2008)
16. J. Gong, J. Wu, Z. Guan, J. Eur. Ceram. Soc. **19**, 2625 (1999)
17. H. Li, R.C. Bradt, J. Mater. Sci. **28**, 917 (1993)
18. S. Cavdar, E. Deniz, H. Koralay, O. Ozturk, M. Erdem, A. Gunen, J. Supercond. Nov. Magn. (2012). doi:10.1007/s10948-012-1629-7
19. H. Li, R.C. Bradt, J. Mater. Sci. **31**, 1065 (1996)
20. K. Sangwal, Mater. Chem. Phys. **63**, 145 (2000)
21. S. Bal, M. Dogruer, G. Yildirim, A. Varilci, C. Terzioglu, Y. Zalaoglu, J. Supercond. Nov. Magn. **25**, 847 (2012)
22. G. Yildirim, M. Dogruer, O. Ozturk, A. Varilci, C. Terzioglu, Y. Zalaoglu, J. Supercond. Nov. Magn. **25**, 893 (2012)
23. E. Asikuzun, O. Ozturk, H.A. Cetinkara, G. Yildirim, A. Varilci, M. Yılmazlar, C. Terzioglu, J. Mater. Sci.: Mater. Electron. **23**, 1001 (2012)
24. O. Ozturk, E. Asikuzun, M. Erdem, G. Yildirim, O. Yildiz, C. Terzioglu, J. Mater. Sci.: Mater. Electron. **23**, 511 (2012)
25. R.R. Reddy, M. Murakami, S. Tanaka, P.V. Reddy, Phys. C **257**, 137 (1996)